



Degradation of thiamethoxam in water by the synergy effect between the plasma discharge and the TiO₂ photocatalysis

Shanping Li*, Xiaohong Cao, Lijun Liu, Xiaolong Ma

School of Environmental Science and Engineering, Shandong University, Jinan 250100, China
Tel./Fax: +86 531 88362872; email: lishanping@sdu.edu.cn

Received 22 September 2013; Accepted 18 November 2013

ABSTRACT

TiO₂ loaded on the honeycomb ceramic was tentatively introduced into dielectric barrier discharge (DBD) in a radial-flow configuration, for plasma-induced photocatalytic degradation of a model organic pollutant thiamethoxam in water. The solution was made to flow as a film over the surface of the honeycomb ceramic, whose hydrophilic force kept the water surface undisturbed by the electrical discharge. This characteristic enabled a reduction of the discharge gap. The results indicated that rate constant of thiamethoxam degradation, energy utilization efficiency of thiamethoxam removal and TOC removal were significantly enhanced due to the synergy effect between the plasma discharge and the TiO₂ photocatalysis. The system could adapt to a wide range of liquid conductivity. The TiO₂ film was calcined at 500°C and the crystal structure of the TiO₂ showed no change after use. Higher concentration of H₂O₂ and ·OH were obtained.

Keywords: Dielectric barrier discharge; TiO₂; Honeycomb ceramic; Thiamethoxam; Degradation

1. Introduction

Neonicotinoids play an important role in agriculture with novel mode of chemistry and action [1,2]. Thiamethoxam [(EZ)-3-(2-chloro-1,3-thiazol-5-yl-methyl)-5-methyl-1,3,5-oxadiazinan-4-ylidene(nitro)amine], a second-generation neonicotinoid, has provided an excellent control of many sucking and chewing pests and also been applied to other aspects such as in pet and seed treatment [3–5]. However, rich leaching capability and poor soil sorption of thiamethoxam cause a potential pollution to surface and underground water [6].

Nowadays, compared with some traditional removal methods, the advanced oxidation processes (AOPs) [7,8] have been emerged as a promising alternative for contaminated water treatment. A common feature of the AOPs is that the production of radicals involves an enormous energy expense. The need of an energy-efficient approach for production reaction radicals has motivated the study on application of plasma. Plasma was produced from the high-voltage electrical discharge at the gas–liquid interface. The process accelerates free electrons and then the high-energy electrons colliding with the ambient molecules to ionize, dissociate or activate them, develop plasma to produce a series of chemically active species (i.e. energized electrons, ·H, ·O, ·OH, ·O₃, H₂O₂, neutral

*Corresponding author.

molecules, ionic species). Simultaneously some physical phenomena occur which are quite similar to UV photolysis, UV radiation, ultrasonic cavitations, supercritical water conditions and shock waves [9]. However, there are some problems when operating the discharge plasma directly in the aqueous, e.g. discharge stability is limited because of the electrodes life (especially under the condition of corona discharge) and discharge way is influenced by liquid conductivity. To avoid these disadvantages, the dielectric barrier discharge (DBD) in which water worked as one of the electrodes was developed [10–12].

What's more, the shortages of DBD include making little use of UV light radiation produced by the discharge [13] and the interference of water surface by vibrating electrostatic field from the high-voltage electrode. TiO_2 is a semiconductor with the band gap of 3.0 eV, and UV light can excite pairs of holes and electrons [14–19], whereas high concentration TiO_2 at high concentration would restrain the UV light radiation and plasma channels formation, resulting in a low removal rate of organic pollutions [20–22]. Honeycomb ceramic can be modified by plasma to strengthen its hydrophilic force [23].

In this paper, we have focused on the study of a special type of plasma DBD reactor, where through the preparation of TiO_2 loaded on the honeycomb ceramic by sol-gel method, and the introduction of the honeycomb ceramic in radial-flow configuration reactor, the efficient utilization of UV, the homogeneity of the plasma discharge and discharge gap has been optimized. Consequently, the plasma DBD reactor was characterized by the discharge gap, the rate constant of thiamethoxam degradation, the energy efficiency for thiamethoxam and TOC removal and the reducing effect of high conductivity on degradation. In addition, the formation of H_2O_2 and $\cdot\text{OH}$ in deionized water during the discharge process was measured.

2. Experimental

2.1. Chemicals

The reagents used in this study were of analytic grade: tetrabutyl titanate (purchased from Guangfu Chemical Industry Co., Ltd.), absolute ethyl alcohol and acetic anhydride (purchased from Tianjin Fuyu Chemical Industry Co., Ltd.), thiamethoxam (purchased from Jinan Pesticide Testing Center), honeycomb ceramic (Al_2O_3 content > 95%, porous size 1 mm, height 10 mm, diameter about 100 mm, purchased from Shanghai Industrial Ceramics Co., Ltd.), Na_2HPO_4 (adjust the solution conductivity).

2.2. Equipment and procedure

The detail steps of preparing the TiO_2 film with sol-gel method was showed as follows:

- (1) Prepare A solution: Put (12–15 mL) tetrabutyl titanate, (48–50 mL) ethyl alcohol and (5–8 mL) acetic anhydride into a beaker, stirring for 30–40 min with the magnetic stirring apparatus.
- (2) Prepare B solution: Put (25–30 mL) ethyl alcohol, (15–20 mL) acetic anhydride and (5–7 mL) into a beaker, stirring for 30–40 min like the step (1).
- (3) Put A solution on the magnetic stirring apparatus and add B solution into the A solution, keep a dropping speed of 1 drop/10 s (to inhibit the hydrolysis rate of tetrabutyl titanate). After B solution was run out, go on stirring for 3–5 min to get the transparent sol.
- (4) Put the dry and clean ceramic into the sol for 5 min, then keep the pulling speed of 2–4 mm/s, stove it for 10 min in the drying oven at 80°C , repeat the procedure for four times.
- (5) Calcine step-by-step in the muffle: heat up from room temperature to 110°C ($0.25^\circ\text{C}/\text{min}$), from 110 to 210°C ($0.25\text{--}0.5^\circ\text{C}/\text{min}$), from 210 to 500°C ($0.5\text{--}1^\circ\text{C}/\text{min}$), keep 500°C for 3–4 h to form TiO_2 film.

The high-voltage power supply (CTP-2000 K) used in present study was the same as that in our previous works [24]. The diagram of experimental set-up is shown in Fig. 1. The system consisted of two elec-

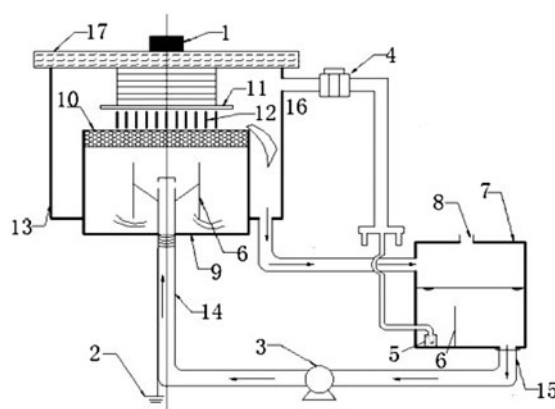


Fig. 1. Experimental set-up: working at normal pressure and temperature. (1) High-voltage; (2) grounding electrode; (3) recirculation pump; (4) air pump; (5) aerator; (6) baffle plate; (7) wastewater tank; (8) vent hole; (9) storage reservoir; (10) honeycomb ceramic; (11) quartz glass plate; (12) plasma zone; (13) overflow tank; (14) inlet tube; (15) water outlet; (16) air outlet and (17) PVC plate.

trodes: the upper metallic electrode and water working as another electrode. The upper metallic electrode was connected to a HV source. The water was in a structure of a flow sedimentation tank (height 700 mm, inner diameter 100 mm and outer diameter 140 mm) and the ground electrode was placed in the centre of the reactor. DBD system was usually with one or two electrodes covered by the isolation medium in the reactor. In this paper, quartz glass (diameter 90 mm) was used as isolation medium and was located below the high-voltage electrode. To improve the experimental set-up, the honeycomb ceramic (height 10 mm, diameter about 100 mm, pore diameter 1 mm) was embedded in the reactor, keeping the upper surface of honeycomb ceramic flush at the top of reactor. After switching on the high-voltage power supply, under the action of the peristaltic pump, the water flowed into the reactor through its bottom, and then to form a water film of about 0.5 mm depth on the ceramic upper surface. The water flow rate was 105 mL/min. The discharge ozone was between the isolation medium and the water film with the discharge gap of 4 mm. The whole experiment was conducted at normal pressure and temperature.

2.3. Analysis

The crystal structure of TiO₂ was identified by X-ray Diffractometer (DD2TD3000), operated over angular ranges of $2\theta = 20\text{--}70^\circ$, scanned at the speed of $0.002^\circ/\text{s}$ and steps of 0.01° . The apparatus was performed at 35 KV and 45 mA. Scanning electron microscope (SEM) was used to observe the surface structure of the TiO₂ film.

Degradation of thiamethoxam was monitored for every 20 min intervals of plasma treatment by UV-vis spectrophotometer (TU-1810) set at 250 nm. The degradation rate was calculated by the following equation:

$$\text{Degradation rate}(\%) = \frac{C_0(\text{mg/L}) - C_t(\text{mg/L})}{C_0(\text{mg/L})} \times 100\% \quad (1)$$

where C_0 and C_t are the concentrations of thiamethoxam at a given reaction time and the initial concentration, respectively.

The TOC of treated water was determined by a total organic carbon analyser (CN61M/GDYS103SY). The liquid conductivity of the solution was measured by a conductivity meter (DDB-303).

The hydrogen peroxide (H₂O₂) produced in the degradation process has been evaluated by the colorimetric method, as reported [25].

In neutral or alkaline solution, the hydrogen peroxide could oxidize the iodine ion. (1) Taking 1 mL samples under different discharge times and adding to 5 mL iodine reagent and 4 mL deionized water. (2) Deionized water worked as the blank sample, determining the absorbency under the wavelength of 350 nm. (3) H₂O₂ concentration was calculated as follows:

$$C = 40 \times d \times A \quad (2)$$

where C is H₂O₂ concentration, mM; d is dilution factor, taking as 10; A is sample absorbance.

OH was determined through chemical method using salicylic acid as the probe [26]. The detail analysis is as follows: (1) using visible-ultraviolet spectrometer to determine the maximum absorption peak of the salicylic; (2) drawing the standard curve of the salicylic; (3) treating the salicylic solution with the plasma discharge and taking the samples every 20 min, determining its absorbency and then to calculate its concentration on the basis of standard curve; (4) according to the reaction equation between hydroxyl radical and salicylic, the hydroxyl radical concentration could be worked out indirectly.

The degradation processes of thiamethoxam conformed to first-order kinetics equation. The kinetic pathway of thiamethoxam degradation could be showed as follows:

$$\ln\left(\frac{C_0(\text{mg/L})}{C_t(\text{mg/L})}\right) = k_{cp}t(\text{min}) \quad (3)$$

where C_0 is the initial concentration; C_t is the concentration of thiamethoxam at a given reaction time; k_{cp} is the rate constant; and t is the degradation time.

To compare the system efficiency under different conditions, the yield values ($Y(\text{g/kWh})$) were introduced [27]. Y presented the amount of thiamethoxam degradation per unit of energy consumed in the system:

$$Y(\text{g/kWh}) = \frac{C_0(\text{mg/L}) \times V(\text{L}) \times \frac{1}{100} \times \text{conv}(\%)}{P(\text{kW}) \times t(\text{min})} \times 60 \times 10^{-3} \quad (4)$$

where C_0 is the initial concentration of thiamethoxam in solution, V is the solution volume, conv is the degradation rate, P is the average power in the discharge and t is the degradation time.

Instantaneous power method was used to determine the discharge power. This method using voltage

probe and current probe measured working voltage and working current waveform of low temperature plasma reactor, then to calculate the instantaneous power curve through digital oscilloscope. According to the power curve, the discharge power could be got.

Thiamethoxam solution of 1,000 mL volume and 100 mg/L concentration was used for the investigation of properties of the experimental set-up. A recirculation pump (BT00-100M) at a speed of 300 mL/min was introduced to provide the circulation water. All the results were got by performing triplicate experiments.

3. Results and discussion

3.1. The characteristic of TiO_2 prepared by gel-sol method

As presented in Fig. 2(a), after the TiO_2 film was calcined at 500°C for 5 h, the main diffraction peak of XRD was at 25.3° , which showed that anatase helping photocatalytic reaction could be got under this condition. The rutile was found at 46.5° and 58.7° , but the proportion was relatively low. The reason why the anatase was better for photocatalytic reaction in comparison to rutile was explained in the following: rutile has the feature of stable crystal shape, good crystal structure, less crystal defect and less oxygen vacancy—the oxygen vacancy is the key of the photocatalytic reaction. Anatase has more oxygen vacancy and its forbidden band width is small (3.0 eV) [28–36]. According to the width of the spectral peak, the particle size could be worked out (20–30 nm). In addition, after the TiO_2 was used in the discharge process, the XRD of TiO_2 did not be changed, so the catalyst could be reused.

From Fig. 2(b), it could be seen that TiO_2 was granular structure (average size 25 nm in diameter). Uniform distribution and rough surface of the TiO_2 particles could not only increase the adsorption quantity of reactants, but also be advantageous to the multiple reflection of UV light on the rough surface. These features increased the light absorption and utilization and conducted an efficient light catalytic reaction. The thickness of the TiO_2 film was about 150 nm.

Fig. 2(c) indicates that the changing of the ceramic contact angle was small without plasma discharge, after the ceramic was modified by the plasma, the contact angle dropped rapidly. The contact angle was close to zero after 16 min, which resulted in a good hydrophilic.

3.2. The discharge gap in the discharge process with/without honeycomb ceramic

According to our previous experiment [37], the minimum discharge gap without honeycomb ceramic

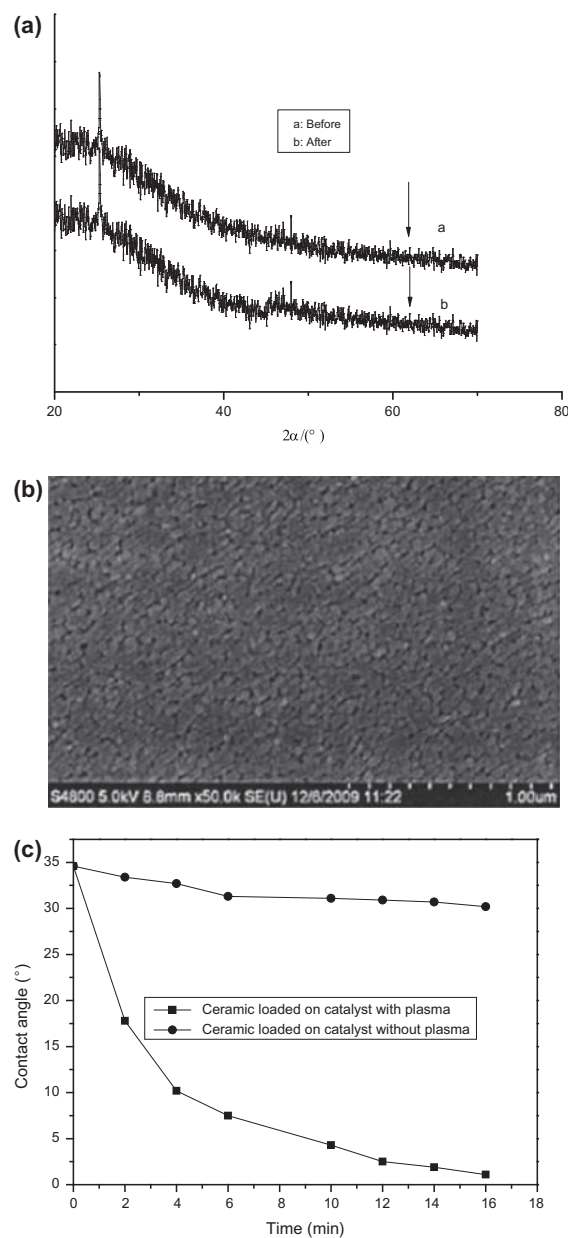


Fig. 2. The characteristic of TiO_2 ; (a) for XRD: angular ranges of $2\theta = 20\text{--}70^\circ$, scanned speed of $0.002^\circ/\text{s}$ and steps of 0.01° , voltage of 35 KV and current of 45 mA; (b) for SEM: current of 50 KV, magnification times of 50; (c) the contact angle for ceramic with/without plasma.

was 8 mm, while the discharge gap in this study was reduced to 5 mm. That was because when the discharge began, the surface of the honeycomb ceramic was modified by the plasma to strengthen its hydrophilic force. The high hydrophilic force could obtain a smaller discharge gap and did not bring the following difficulties: (1) make the water surface sucked up to the electrode with the electrostatic field existing; (2)

cause the discharge set-up short circuit like before. Under the same degradation rate and discharge power, the improved experimental set-up with a narrower discharge gap, which resulted in a shorter discharge time and a higher yield values, is shown in Table 1.

3.3. Degradation and mineralization of thiamethoxam in the discharge process with/without honeycomb ceramic

In order to investigate the effect of experiment set-up with honeycomb ceramic on the degradation and mineralization of thiamethoxam solution, thiamethoxam removal and TOC removal were discussed. The experiment with/without ceramic was conducted for the same discharge gap and discharge power. As presented in Fig. 3(a), the experiment set-up with honeycomb ceramic has a faster degradation rate of thiamethoxam than that without honeycomb ceramic, after 160 min degradation, the removal rates were 85.875 and 68.540%, respectively. In addition, according to Eq. (4), the yield values (Y) could be calculated out. In the equation, with/without honeycomb the C_0 , V and t were the same, what is more, we made the two P be essentially same by adjusting the input voltage and current. The yield values for thiamethoxam removal with honeycomb ceramic (9.0×10^{-3} g/kWh) were over two times greater than that without honeycomb ceramic (3.6×10^{-3} g/kWh). Y presented that how many thiamethoxam were removed when the system consumed one kilowatt hour electricity. The bigger the Y was, the more thiamethoxam was degraded by consuming one kilowatt hour electricity.

And also the rate constant was improved to surpass one and a half times with honeycomb ceramic in DBD process, compared with previous apparatus, from $8.3 \times 10^{-3} \text{ min}^{-1}$ ($R^2=0.9891$) without honeycomb ceramic to $1.3 \times 10^{-2} \text{ min}^{-1}$ ($R^2=0.9916$) with honeycomb ceramic. Both of the processes fitted a first-order-rate kinetics suggesting a liner relationship between the thiamethoxam concentration and degradation time.

Fig. 3(b) indicated that (1) in the early 40 min, the adsorption on the catalyst had a little influence on

thiamethoxam degradation (about 9% removal rate), the absorption equilibrium was achieved after only 40 min; (2) the DBD with ceramic (no supporting catalyst) had a 73.734% degradation on thiamethoxam, which was lower than that of DBD with ceramic, but was higher than that of DBD without ceramic. A comparison between the DBD (with ceramic) and the DBD (with ceramic (no supporting catalyst)), the degradation of catalyst could be found.

Moreover, Fig. 3(c) showed the mineralization of thiamethoxam with/without honeycomb ceramic in the DBD experiment set-up. The TOC removal of thiamethoxam was obviously increased by about 20%.

In addition, the pyrolysis effect on degradation and mineralization of thiamethoxam cannot be neglected. During the discharge process, much thermal was released and made the solution temperature, which accelerated the molecular motion and improved the degradation efficiency.

3.4. Higher initial liquid conductivity for thiamethoxam degradation in the DBD process with/without honeycomb ceramic

To study the effect of improved apparatus on thiamethoxam degradation under a higher initial liquid conductivity (350–400 $\mu\text{s/cm}$), the experiment was conducted, as shown in Fig. 4. Whether the honeycomb ceramic was introduced in the DBD process or not, the speed of thiamethoxam degradation under higher liquid conductivity was always lower than that under low liquid conductivity. It was because that the higher liquid conductivity would change the discharge way [38] and was bad for the organics degradation. The rate constant for thiamethoxam degradation at 350–400 $\mu\text{s/cm}$ without honeycomb ceramic was $7.5 \times 10^{-3} \text{ s}^{-1}$, which was less than $8.3 \times 10^{-3} \text{ s}^{-1}$ for low liquid conductivity (5–7 $\mu\text{s/cm}$). Meanwhile, the rate constant for thiamethoxam degradation at high liquid conductivity with honeycomb ceramic was $1.17 \times 10^{-1} \text{ s}^{-1}$, which was less than $1.35 \times 10^{-1} \text{ s}^{-1}$ for low liquid conductivity. It was indicated that high liquid conductivity had an unfavourable effect on the removal of thiamethoxam with/without honeycomb ceramic.

Table 1
The discharge parameters of the discharge set-up with/without honeycomb ceramic

Experiment condition	Degradation rate (%)	Degradation power (W)	Degradation gap (mm)	Degradation time (min)	Y (g/kWh)
Without honeycomb ceramic	60	100	8	100	3.6×10^{-3}
With honeycomb ceramic	60	100	5	40	9.0×10^{-3}

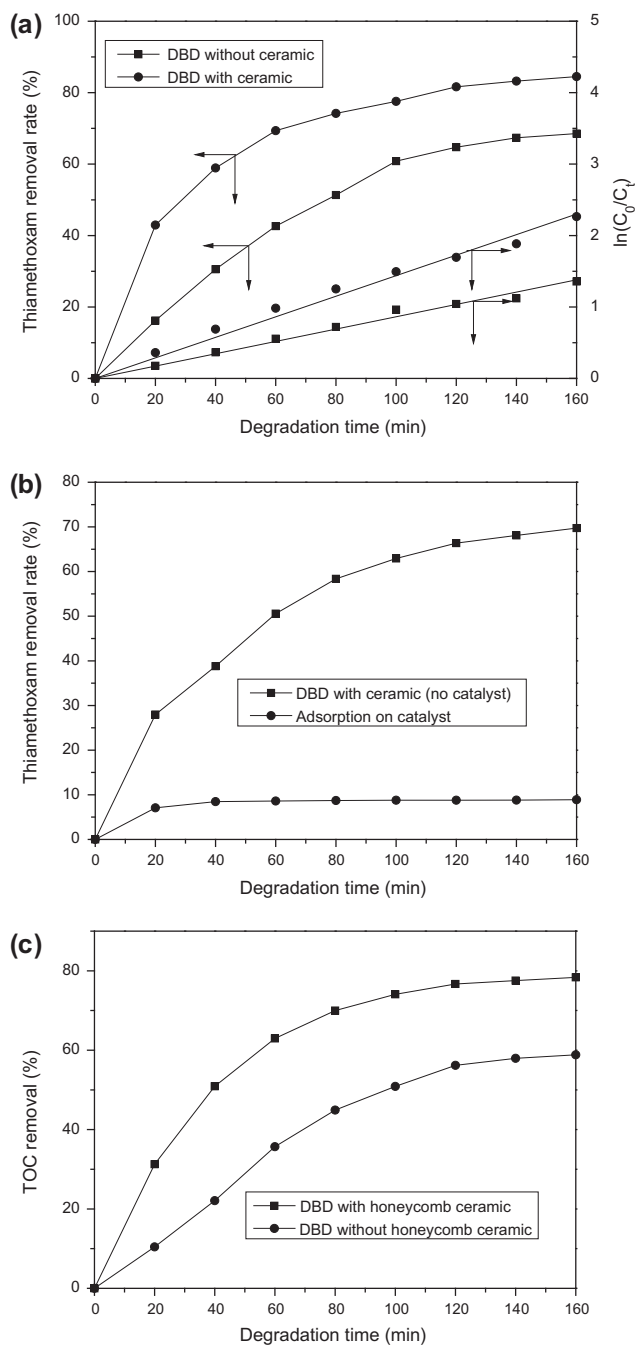


Fig. 3. Degradation and mineralization of thiamethoxam in the DBD process with/without honeycomb ceramic: (a) degradation of thiamethoxam; (b) mineralization of thiamethoxam: discharge voltage = 75 V, discharge gap = 3 mm, pH = 6.67, solution concentration = 100 mg/L, solution volume = 1,000 mL, solution conductivity = 5–7 $\mu\text{s}/\text{cm}$, discharge time = 160 min, sampling time = interval 20 min.

However, the introduction of honeycomb ceramic could reduce the effect on the thiamethoxam degradation.

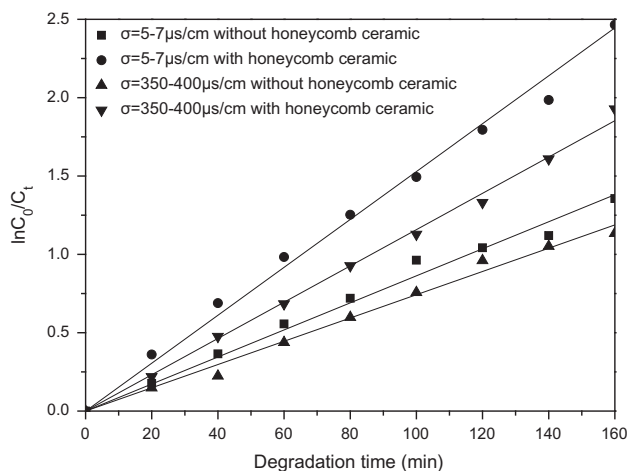


Fig. 4. Higher initial liquid conductivity for thiamethoxam degradation in the DBD process with/without honeycomb ceramic: discharge voltage = 75 V, solution volume = 1,000 mL, solution conductivity = 5–7/350–400 $\mu\text{s}/\text{cm}$ (both follow the first-order-kinetics equation), the rate constants of 350–400 $\mu\text{s}/\text{cm}$ with/without honeycomb ceramic were 1.17×10^{-1} and $7.5 \times 10^{-3} \text{ s}^{-1}$, the rate constant of 5–7 $\mu\text{s}/\text{cm}$ with/without honeycomb ceramic were 1.35×10^{-1} and $8.3 \times 10^{-3} \text{ s}^{-1}$.

3.5. The formation of H_2O_2 and $\cdot\text{OH}$ in deionized water during the discharge process with/without honeycomb ceramic

As Fig. 5 showed, the DBD with honeycomb ceramic could generate a large amount of $\cdot\text{OH}$ and H_2O_2 during the discharge process in deionized water. When the experiment conducted 160 min, the concentrations of $\cdot\text{OH}$ and H_2O_2 were 5.038 mM and 4.497 mM, respectively. In the early 80 min, the concentration of $\cdot\text{OH}$ was higher than that of H_2O_2 , after 80 min this tendency was inverted. That was because with the increase of $\cdot\text{OH}$, they reacted each other to generate H_2O_2 . The formation mechanism of H_2O_2 and $\cdot\text{OH}$ was as follows [39–42]:



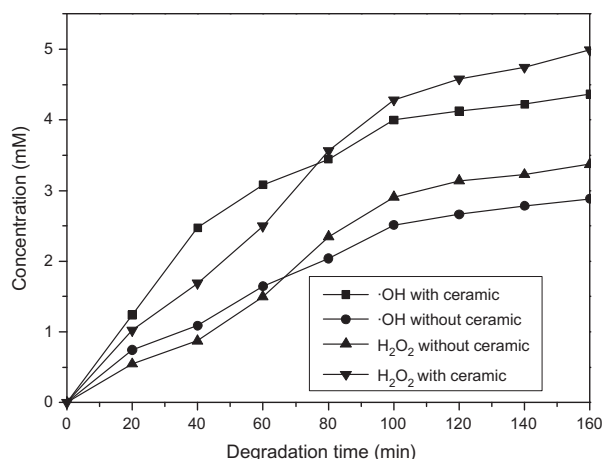
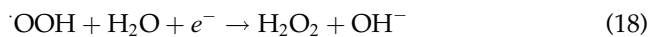
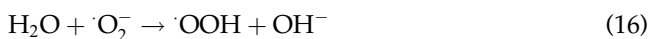
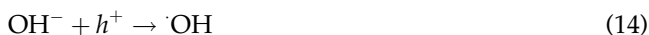
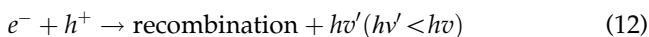
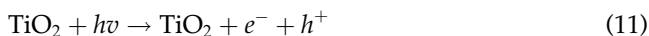


Fig. 5. The formation of H₂O₂ and ·OH during the discharge process with/without honeycomb ceramic: discharge voltage = 75 V, discharge gap = 3 mm, solution volume = 1,000 mL, discharge time = 160 min, sampling time = interval 20 min.



4. Conclusions

The DBD system was improved by the introduction of a honeycomb ceramic with TiO₂ film prepared through sol-gel method into the radial flow reactor. On the one hand, the hydrophilic behaviour of the honeycomb ceramic could keep water surface undisturbed by the electrostatic field force and enabled the increase in homogeneity and stability of the discharge process. On the other hand, the photocatalytic reaction of TiO₂ promoted thiamethoxam degradation. In addition, the rate constant of

thiamethoxam degradation, energy efficiency for thiamethoxam removal and TOC removal were obviously improved and the system had a good degradation of thiamethoxam in a wide range of liquid conductivity. The formation of H₂O₂ and ·OOH in deionized water during the discharge process was enhanced.

Acknowledgements

This work was supported by the National Eleventh-five Year Science and Technology Supporting Program of China (2006BAJ05A12) and the Science and Technology Development Plan Project of Shandong Province (2011GSF11602).

References

- [1] P. Maienfisch, M. Angst, F. Brandl, W. Fischer, D. Hofer, H. Kayser, W. Kobel, A. Rindlisbacher, R. Senn, A. Steinemann, H. Widmer, Chemistry and biology of thiamethoxam: A second generation neonicotinoid, *Pest Manag. Sci.* 57 (2001) 906–913.
- [2] A.P.F.M. de Urzedo, M.E.R. Diniz, C.C. Nascentes, R.R. Catharino, M.N. Eberlin, R. Augusti, Photolytic degradation of the insecticide thiamethoxam in aqueous medium monitored by direct infusion electrospray ionization mass spectrometry, *J. Mass Spectrom.* 42 (2007) 1319–1325.
- [3] S. Dilli Ram, O.P. Lal, Bio-efficacy of thiamethoxam in comparison to recommended insecticides against leafhopper and white fly of brinjal (*Solanum melongena* L.), *J. Entomol. Res.* 26 (2002) 257–262.
- [4] H.P. Misra, B. Senapati, Evaluation of new insecticides against okra jassid (*Amrasca biguttula*), *Indian J. Agric. Sci.* 73 (2003) 576–578.
- [5] A. Elbert, M. Haas, B. Springer, Applied aspects of neonicotinoid uses in crop protection, *Pest Manag. Sci.* 64 (2008) 1099–1105.
- [6] P. Correia, R.A.R. Boaventura, M.A.M Reis, Effect of operating parameters on molinate biodegradation, *Water Res.* 40 (2006) 331–340.
- [7] F.J. Javier Benitez, J.L. Acero, F.J. Real, Degradation of carbofuran by using ozone, UV radiation and advanced oxidation processes, *J. Hazard. Mater.* 89 (2002) 51–65.
- [8] R. Venkatadri, R.W. Peters, Chemical oxidation technologies: Ultraviolet light/hydrogen peroxide, fenton's reagent, and titanium dioxide-assisted photocatalysis, *Hazard. Waste Hazard. Mater.* 10 (1993) 107–149.
- [9] M.A. Malik, Synergistic effect of plasmacatalyst and ozone in a pulsed corona discharge reactor on the decomposition of organic pollutants in water, *Plasma Sour. Sci. Technol.* 12 (2003) S26–S32.
- [10] M.M. Kuraica, B.M. Obradović, D. Manojlović, D.R. Ostojić, J. Purić, Ozonized water generator based on coaxial dielectric-barrier-discharge in air, *Vacuum* 73 (2004) 705–708.
- [11] J. Velikonja, M.A. Bergougnou, G.S.P. Castle, W.L. Caims, I.I. Inculet, Co-generation of ozone and hydrogen peroxide by dielectric barrier AC discharge in humid oxygen Ozone, *Sci. Eng.* 23 (2001) 467–478.

- [12] H. Sekiguchi, K. Yamagata, Effect of liquid film on decomposition of CFC-12 using dielectric barrier discharge, *Thin Solid Films* 457 (2004) 34–38.
- [13] W.S. Perkins, Oxidative decoloration of dyes in aqueous medium, *Text. Chem. Color.* 1 (1999) 33–37.
- [14] A. Fujishima, T.N. Rao, D.A. Tryk, Titanium dioxide photocatalysis, *J. Photochem. Photobiol. C: Photochem. Rev.* 1 (2000) 1–21.
- [15] C. Liu, X.H. Tang, C.H. MO, J. Wang, Characterization and photocatalytic activity of Ni doped TiO₂ nano photocatalysts prepared by low temperature combustion synthesis, *Environ. Sci.* 26 (2006) 2150–2153.
- [16] S. Luo, Z. Tang, W. Yao, Z. Zhang, Low-temperature combustion synthesis and characterization of nano-sized tetragonal barium titanate powders, *Microelectron. Eng.* 66 (2003) 147–152.
- [17] Wei Zhao, Wanhong Ma, Chunheng Chen, Jincai Zhao, Zhigang Shuai, Efficient degradation of toxic organic pollutants with Ni₂O₃/TiO₂-xB_x under visible irradiation, *J. Am. Chem. Soc.* 126 (2004) 4728–4783.
- [18] Di Li, H. Haneda, S. Hishita, N. Ohashi, Visible-light-driven nitrogen-doped TiO₂ photocatalysts: Effect of nitrogen precursors on their photocatalysis for decomposition of gas-phase organic pollutants, *Mater. Sci. Eng. B* 117 (2005) 67–75.
- [19] R. Asahi, T. Morikawa, T. Ohwaki, K. Aoki, Y. Taga, Visible-Light photocatalysis in nitrogen-doped titanium oxides, *Science* 293 (2001) 269–271.
- [20] X.L. Hao, M.H. Zhou, L.C. Lei, Non-thermal plasma-induced photocatalytic degradation of 4-chlorophenol in water, *J. Hazard. Mater.* 141 (2007) 475–482.
- [21] P. Lukes, M. Clupek, P. Sunka, F. Peterka, T. Sano, N. Negishi, S. Matsuzawa, K. Takeuchi, Degradation of phenol by underwater pulsed corona discharge in combination with TiO₂ photocatalysis, *Res. Chem. Intermediat.* 31 (2005) 285–294.
- [22] W. Choi, A. Termin, M.R. Hoffmann, The role of metal ion dopants in quantum-sized TiO₂: Correlation between photoreactivity and charge carrier recombination dynamics, *J. Phys. Chem.* 98 (1994) 13669–13679.
- [23] M.L. Steen, L. Hymas, E.D. Havey, N.E. Capps, D.G. Castner, E.R. Fisher, Low temperature plasma treatment of asymmetric polysulfone membranes for permanent hydrophilic surface modification, *J. Membrane Sci.* 188 (2001) 97–114.
- [24] S.P. Li, Y.Y. Jiang, X.H. Cao, Degradation of nitenpyram pesticide in aqueous solution by low-temperature plasma, *Environ. Technol.* 34 (2013) 1609–1616.
- [25] G. Eisenberg, Colorimetric determination of hydrogen peroxide, *Ind. Eng. Chem. Anal. Ed.* 15 (1943) 327–328.
- [26] W.U. Jian-lin, Y.U.A.N. Li, M.A.O. Xue-feng, F.U. Yan, G.A.O. Jin-zhang, Determination of hydroxyl radical produced by glow discharge plasma with salicylic acid trapping, *J. Northwest Normal Univ.* 43 (2007) 53–56.
- [27] M. Magureanu, D. Piroi, N.B. Mandache, V. David, A. Medvedovici, V.I. Parvulescu, Degradation of pharmaceutical compound pentoxifylline in water by non-thermal plasma treatment, *Water Res.* 44 (2010) 3445–3453.
- [28] A.L. Linsebigler, G. Lu, J.T. Yates Jr., Photocatalysis on TiO₂ surfaces: Principles, mechanisms, and selected results, *Chem. Rev.* 95 (1995) 735–758.
- [29] W. Choi, A. Termin, M.R. Hoffmann, The role of metal ion dopants in quantum-sized TiO₂: Correlation between photoreactivity and charge carrier recombination dynamics, *J. Phys. Chem.* 98 (1994) 13669–13679.
- [30] Y. Liang, H. Wang, H. Sanchez Casalongue, Z. Chen, H. Dai, TiO₂ nanocrystals grown on graphene as advanced photocatalytic hybrid materials, *Nano Res.* 3 (2010) 701–705.
- [31] H. Wang, Nanocrystal growth on graphene with various degrees of oxidation, *J. Am. Chem. Soc.* 132 (2010) 3270–3271.
- [32] Y. Si, E.T. Samulski, Exfoliated graphene separated by platinum nanoparticles, *Chem. Mater.* 20 (2008) 6792–6797.
- [33] D.H. Lee, J.E. Kim, T.H. Han, J.W. Hwang, S. Jeon, S.-Y. Choi, S.H. Hong, W.J. Lee, R.S. Ruoff, S.O. Kim, Versatile carbon hybrid films composed of vertical carbon nanotubes grown on mechanically compliant graphene films, *Adv. Mater.* 22 (2010) 1247–1252.
- [34] H. Wang, Ni(OH)₂ nanoplates grown on graphene as advanced electrochemical pseudocapacitor materials, *J. Am. Chem. Soc.* 132 (2010) 7472–7477.
- [35] E.J. Yoo, T. Okata, T. Akita, M. Kohyama, J. Nakamura, I. Honma, Enhanced electrocatalytic activity of Pt subnanoclusters on graphene nanosheet surface, *Nano Lett.* 9 (2009) 2255–2259.
- [36] A. Murugan, T. Muraliganth, A. Manthiram, Rapid, facile microwave-solvothermal synthesis of graphene nanosheets and their polyaniline nanocomposites for energy storage, *Chem. Mater.* 21 (2009) 5004–5006.
- [37] S.P. Li, J.J. Cui, Y.Y. Jiang, Study of using low-temperature plasma to degrade nitenpyram pesticide in aqueous solution, *High Voltage Engineer.* 37 (2011) 2517–2522.
- [38] B. Sun, M. Sato, J.S. Sid Clements, Optical study of active species produced by a pulsed streamer corona discharge in water, *J. Electrostat.* 39 (1997) 189–202.
- [39] D. Ravelli, D. Dondi, M. Fagnoni, A. Albini, Photocatalysis. A multi-faceted concept for green chemistry, *Chem. Soc. Rev.* 38 (2009) 1999–2011.
- [40] K. Woan, G. Pyrgiotakis, W. Sigmund, *Adv. Mater.* 21 (2009) 2233–2239.
- [41] X.H. Wang, J.G. Li, H. Kamiyama, Y. Moriyoshi, T. Ishigaki, Wavelength-sensitive photocatalytic degradation of methyl orange in aqueous suspension over iron(III)-doped TiO₂ nanopowders under UV and visible light irradiation, *Phys. Chem.* 110 (2006) 6804–6809.
- [42] W. Wang, P. Serp, Photocatalytic degradation of phenol on MWNT and titania composite catalysts prepared by a modified sol-gel method, *Appl. Catal.* 56 (2005) 305–312.